17

# AN ISOCHRONAL ANNEALING STUDY OF THE KINETICS OF VO AND $VO_2$ DEFECTS IN NEUTRON IRRADIATED SI

C. A. LONDOS, N. V. SARLIS AND L. G. FYTROS
*University of Athens, Physics Department, Solid State Section*
*Panepistimiopolis, Zografos, Athens 157 84 Greece*

**Abstract.** The infrared spectra of room-temperature, neutron-irradiated, Czochralski-grown Si were investigated. During the anneal, the 827 $cm^{-1}$ VO defect band decreases, and another band at 885 $cm^{-1}$ of $VO_2$ centres increases. The kinetics of the evolution of these two defects was investigated. The decay of VO is dominated by a second order reaction ($VO + Si_i \rightarrow O_i$) with an activation energy 1.70 eV. The growth of $VO_2$ exhibits two stages. Below 360 °C, a first order reaction ($VO + O_i \rightarrow VO_2$) with an activation energy of 1.46 eV is more likely to occur. Above 360 °C, the growth of $VO_2$ seems to be correlated with mechanisms which do not involve VO centres. This behaviour may become explicable, at least qualitatively, in terms of a mechanism that involves the formation of oxygen dimers.

## 1. Introduction

Radiation-induced defects in Si have been the subject of many investigations, and numerous experimental and theoretical works have been reported so far. The A-centre (VO) is one of the most common defects encountered in irradiated Si. It is registered in all electrical ($E_c - 0.17$ eV level) and/or optical (827 $cm^{-1}$ LVM) studies irrespective of the kind of irradiation (*e.g.* electrons, protons, neutrons, $\alpha$-particles, $\gamma$-rays, *etc.*) Although a lot of information has been gathered about the structure and the electronic and optical properties of the centre, its exact annealing behaviour has not been completely clarified so far. The main reason for this is that the annealing of A-centres can follow simultaneously more than one reaction channel. Among them are the following:



*R. Jones (ed.), Early Stages of Oxygen Precipitation in Silicon, 477–484.*
© 1996 *Kluwer Academic Publishers. Printed in the Netherlands.*

i) Dissociation of A-centres

$$VO \rightarrow V + O_i, \tag{1}$$

ii) Destruction of A-centres by silicon self-interstitials emitted from defect clusters

$$VO + Si_i \rightarrow O_i, \tag{2}$$

iii) Association of VO with $O_i$ atoms

$$VO + O_i \rightarrow VO_2, \tag{3}$$

and/or with another VO centre

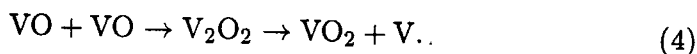

$$VO + VO \rightarrow V_2O_2 \rightarrow VO_2 + V.. \tag{4}$$

In principle, all these processes could occur in parallel. However it depends on the dose and the kind of irradiation, the oxygen content of the material, the temperature, *etc.*, as to which mechanism will prevail. It is therefore evident that the annealing process of the A-centre is compounded and complicated. Consequently, experimental data should be treated very carefully in order to distinguish the effect of the various processes and avoid misleading conclusions. Activation energies for example, reported from Arrhenius plots where only one process has been considered, may not represent true values if one or more competing processes with different activation energies occur in parallel. The scatter of reported values of activation energies cited in the literature reflects the above complexities as a result of the fact that a consensus among researchers has not been reached concerning the exact kinetics describing the phenomenon [1, 2, 3, 4].

In IR studies the decay of the 827 $cm^{-1}$ signal from A-centres is accompanied by the growth of an 885 $cm^{-1}$ signal attributed to $VO_2$ defects [2]. In this paper we shall examine the annealing kinetics of A-centres and the correlated growth kinetics of $VO_2$ defects using data taken from isochronal annealing studies of fast neutron irradiated Cz-grown Si. We shall consider mainly two scenaria of combining processes for the decay of VO and the growth of $VO_2$ defects in an attempt to establish which are the most suitable, but also physically meaningful mechanisms, that explain the whole phenomenon.

## 2. Experimental

Cz-grown Si samples with undetactable levels of substitutional carbon $C_s$ ($[C_s] < 10^{16}$ $cm^{-3}$) and $[O_i] \approx 10^{18}$ $cm^{-3}$ were irradiated ($T_{irr} < 50\,°C$) by fast neutrons at a dose equal to $10^{17}$ $cm^{-2}$. The samples were wrapped in

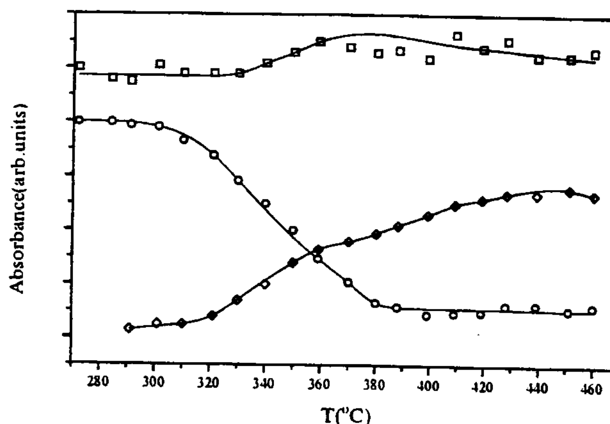


*Figure 1.* The evolution of VO (circles) and $VO_2$ (rhombs) defects as a function of temperature (15 min. isochronal annealing). The variation of $O_i$ (squares) is also shown.

Cd foils to eliminate the effect of thermal neutrons. The heat treatments for annealing studies were carried out in open furnaces. The infrared absorption spectra were recorded at room temperature by using a JASCO-IR 700 dual beam spectrometer. Control samples of equal thickness from Float-Zone material were used during the measurements in order to subtract the two-phonon inherent absorption of the Si lattice.

## 3. Experimental Results and Discussion

As expected, the A-centre band at 827 $cm^{-1}$ appears in our IR spectra, immediately after irradiation. On increasing the temperature as the isochronal anneal is carried out, the shape of the band is distorted by the emergence of satellite bands previously reported in the literature [5]. To extract the individual contribution of each component, the data were analyzed by computer deconvolution using Lorentzian profiles for each band [6]. Figure 1 shows the annealing behaviour of the A-centre band after subtracting the contributions of the satellite bands. The growth of the 885 $cm^{-1}$ band attributed to $VO_2$ centre is also shown. The study of the evolution of these two defects will be the subject of this investigation.

### 3.1. THE DECAY OF VO

As it was already mentioned there are many reactions, Equations (1)–(4), that could take place in this temperature range. However, the irradiation is rather heavy and the isochronal annealing time $\tau = 15$ min. is rather small.

One would expect therefore, that the contribution of some of the reactions will be negligible in comparison with some others [3].

Since in neutron-irradiated Si large defect clusters are formed which liberate $Si_i$, in the temperature range under consideration, the most likely process for the decay of VO is that corresponding to equation (2), in agreement with the increase of the $O_i$ concentration shown in figure 1. The process is generally described by a rate equation

$$\frac{d[VO]}{dt} = -k_1 [VO] [Si_i], \tag{5}$$

which may be approximated for the purposes of the present analysis, by

$$\frac{d[VO]}{dt} = -k_1 [VO]^2. \tag{6}$$

By integration, one gets

$$[VO](t) = \frac{[VO]_0}{1 + [VO]_0 \, k_1 \, t}, \tag{7}$$

and

$$k_1 \tau = \frac{1}{[VO]'} - \frac{1}{[VO]_0}, \tag{8}$$

where $k_1$ has a temperature dependence of the form $k_1 \propto e^{-E_a/kT}$, $E_a$ being the activation energy, $[VO]_0$ is the initial concentration of A-centres, $[VO]'$ the concentration of VO after annealing for time $\tau$ at temperature $T$, and $[VO](t)$ the concentration of VO at any time during the isochronal annealing at $T$. By fitting $\ln k_1$ versus $1/T$ in the range 310–380 °C (figure 2), we find an activation energy $E_a = 1.70 \pm 0.05$ eV with a correlation coefficient $r = 0.997$. Since the value inferred by the fitting differs from the true mean value of $\ln k_1$ that would have been obtained by an infinite number of experiments, we plot in figure 2 the 80% confidence interval curves [7]. This means, that according to the fitting, the true mean value of $\ln k_1$ has an 80% probability of lying inside the area enclosed by the 80% confidence interval curves.

### 3.2. THE GROWTH OF $VO_2$

Evidently, from figure 1 the growth of $VO_2$ is related to the decay of A-centres. This relation may be modelled by combining equation (2) either with equation (3) or with equation (4).

#### 3.2.1. *Scenario I*

In the first alternative the production of $VO_2$ is a first order process

$$\frac{d[VO_2]}{dt} = -k_2 [VO], \tag{9}$$

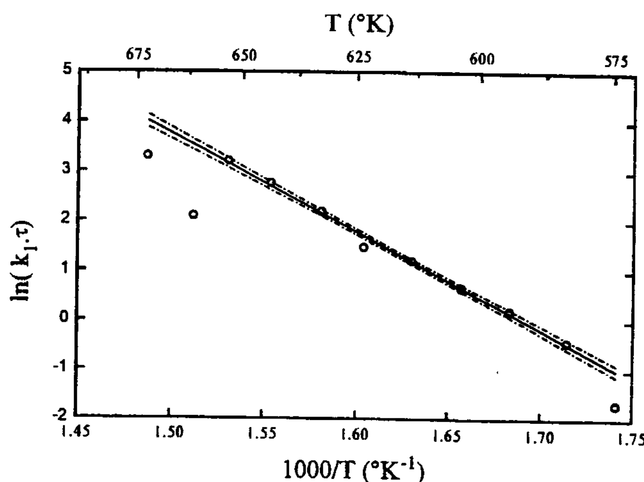


*Figure 2.* The Arrhenius plot for the decay of VO; the 80% confidence interval is enclosed by the two lateral curves.

where $[VO](t)$ is given by equation (7). By integration, one gets

$$k_2 = k_1 \frac{[VO_2]' - [VO_2]_0}{\ln([VO]_0 / [VO]')}, \tag{10}$$

where $[VO_2]_0$ and $[VO_2]'$ are defined in the same way as $[VO]_0$ and $[VO]'$ respectively. By subsituting equation (8) into (10) the following expression for $k_2$ is obtained

$$k_2 \tau = \left(\frac{1}{[VO]'} - \frac{1}{[VO]_0}\right) \frac{[VO_2]' - [VO_2]_0}{\ln([VO]_0 / [VO]')}. \tag{11}$$

The Arrhenius plot for the rate constant $k_2$ is shown in figure 3. As it is seen from this graph two stages possibly exist. In the first stage, below 360 °C, the logarithm of the rate constant can be fitted to a linear expression of $1/T$, and an activation energy of $E_a = (1.46 \pm 0.29)$ eV is obtained, with a correlation coefficient r = 0.962. In figure 3, the 80% confidence interval curves are also shown [7].

### 3.2.2. *Scenario II*

In the second alternative, the production of $VO_2$ is a second order process,

$$\frac{d[VO_2]}{dt} = -k_2' [VO]^2, \tag{12}$$

where $[VO](t)$ is given by equation (7). By integration one gets

$$k_2' = k_1 \frac{[VO_2]' - [VO_2]_0}{[VO]_0 - [VO]'}. \tag{13}$$

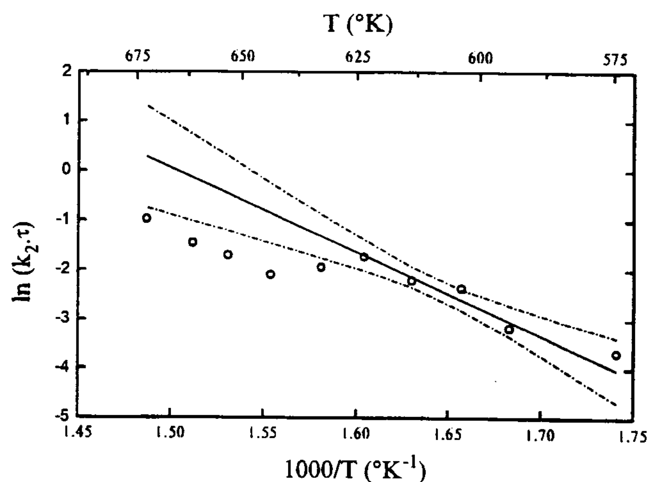


*Figure 3.* The Arrhenius plot for the growth of $VO_2$ (first order kinetics); the 80% confidence interval is enclosed by the two lateral curves.

By subsituting equation (8) into (14) the following expression for $k_2'$ is obtained

$$k_2'\tau = \left(\frac{1}{[VO]'} - \frac{1}{[VO]_0}\right) \frac{[VO_2]' - [VO_2]_0}{[VO]_0 - [VO]'}. \qquad (14)$$

The Arrhenius plot for the rate constant $k_2'$ is shown in figure 4. We observe again the existence of two characteristic stages below and above 360 °C. The activation energy, extracted from fitting the data of the first stage, has a value $E_a = (1.96 \pm 0.27)$ eV, with a correlation coefficient r = 0.981. In figure 4, the 80% confidence interval curves are also shown [7].

Let us consider now the second stage, above 360 °C, of the growth of $VO_2$. As it is seen from both figures 3 and 4, experimental points lie outside the 80% confidence interval curves for temperatures in this range. In other words, the experimental values of $\ln k_2$ or $\ln k_2'$ are not described adequately by the regression lines. Moreover, for temperatures above 380 °C, we notice that $VO_2$ continues to grow (figure 1), although the VO signal has almost stabilized at low amplitudes. These observations imply that another mechanism for the formation of $VO_2$ is involved. One possibility is through oxygen dimers. The notion of oxygen dimers that would migrate more easily than oxygen interstitials atoms through the Si lattice was firstly proposed by Gösele and Tan in order to explain experimental data concerning thermal donor behaviour [8]. The idea was also used to suggest an alternative process for $VO_2$ formation as a result of lattice vacancy trapping by oxygen dimers [9]. Such an explanation could account – at least qualitatively – for our experimental observations too. Notably, the oxygen concentration in figure 1 shows a tendency to decrease

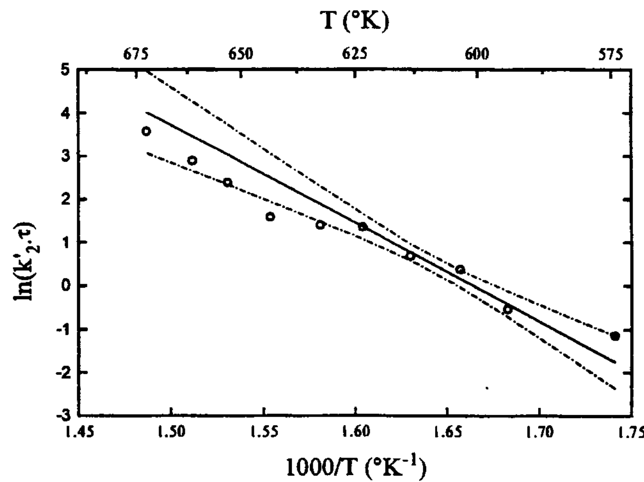


*Figure 4.* The Arrhenius plot for the growth of $VO_2$ (second order kinetics); the 80% confidence interval is enclosed by the two lateral curves.

in this temperature range, a fact which is in accord with processes involving oxygen dimerization. Quantitatively, however, the picture is not so clear. A more detailed report on the variation of $O_i$ concentration and its relation to the processes of formation of the various $VO_n$ defects in Si will be published shortly [10].

### 3.3. RECAPITULATION

The results are summarized in Table 1. Although scenario II exhibits a

TABLE 1. The two scenaria for the decay of VO and $VO_2$.

| | Scenario I | Scenario II |
|---|---|---|
| Reactions | $VO + Si_i \rightarrow O_i$ | $VO + Si_i \rightarrow O_i$ |
| | $VO + O_i \rightarrow VO_2$ | $VO + VO \rightarrow VO_2 + V$ |
| Rate Equations | $d[VO]/dt = -k_1\,[VO]^2$ | $d[VO]/dt = -k_1\,[VO]^2$ |
| | $d[VO_2]/dt = -k_2\,[VO]$ | $d[VO_2]/dt = -k'_2\,[VO]^2$ |
| Activation Energies | $E_{a1} = (1.70 \pm 0.05)$ eV | $E_{a1} = (1.70 \pm 0.05)$ eV |
| | $E_{a2} = (1.46 \pm 0.29)$ eV | $E_{a2'} = (1.96 \pm 0.27)$ eV |
| Correlation Coefficients | $r_1 = 0.997$ | $r_1 = 0.997$ |
| | $r_2 = 0.962$ | $r_{2'} = 0.981$ |

higher correlation coefficient, scenario I is more likely to occur in our

opinion, since $[O_i]$ is about two orders of magnitude higher than [VO] and therefore reaction (3) is expected to dominate over reaction (4).

## 4. Conclusions

Two scenaria have been employed for the study of the decay of VO and the correlated growth of $VO_2$ defects. In both cases the disappearance of A-centres was studied in terms of annihilation of VO by Si self-interstitials liberated from defect clusters that are expected to be present in neutron-irradiated material. The growth of $VO_2$ exhibits two stages. In the first stage, the growth was discussed in terms of either $O_i$ being trapped by VO (equation 3), or VO defects pairing up to form $V_2O_2$ defects which in turn decompose into $VO_2$ and V (equation 4). In our opinion, a defect reaction model postulating the processes $VO + Si_i \rightarrow O_i$ and $VO + O_i \rightarrow VO_2$ is more physically meaningful due to the high oxygen content of the Si material. In the second stage, the growth is likely to be related to oxygen dimer formation. Fast moving oxygen dimers provide an alternative channel for the creation of $VO_2$ defects through capturing of free lattice vacancies.

## Acknowledgments

N.V.S. was supported by a grant of the National Scholarship Foundation of Greece, IKY.

## References

1. Benski, G., and Augestiniak, W. M. (1957) Annealing of electron bombardment damage in silicon crystals, *Phys. Rev.* **108**, 645–648.
2. Corbett, J. W., Watkins, G. D., and McDonald, R. C. (1964) New oxygen infrared bands in annealed irradiated silicon, *Phys. Rev.* **135**, A1381–A1385.
3. Svensson, B. G., and Lindström, J. L. (1986) Kinetic study of the 830 and 889 $cm^{-1}$ infrared bands during annealing of irradiated silicon, *Phys. Rev. B* **34**, 8709–8717.
4. Tipping, A. K., Newmann, R. C., Newton, D. C., and Tucker, J. H. (1986) Enhanced oxygen diffussion in silicon at low temperatures, in J. von Bardeleben (ed.), *Defects in Semiconductors Materials Science Forum* **10–12**, pp. 887–892.
5. Ramdas, A. K., and Rao, M. G. (1966) Infrared Absorption spectra of oxygen-defect complexes in irradiated Silicon, *Phys. Rev.* **142**, 451–456.
6. Londos, C. A., Sarlis, N. V., Georgiou, G., and Fytros, L. G. (unpublished data).
7. Crow, E. L., Davis, A. F., and Maxfield, M. W. (1960) *Statistics Manual*, Dover Publications, Inc., New York.
8. Gösele, U., and Tan, T. Y. (1982) Oxygen diffusion and thermal donor formation in silicon, *Appl. Phys. A* **28**, 79–92.
9. Svenson, B. G., and Lindström, J. L. (1985) Growth of the 889 $cm^{-1}$ infrared band in annealed electron-irradiated Si, *Appl. Phys. Lett.* **47**, 841–843.
10. Sarlis, N. V., Londos, C. A., and Fytros, L. G. (to be published).